ELSEVIER

Applied Surface Science 96–98 (1996) 332–340

applied surface science

Laser damage of $CaF_2(111)$ surfaces at 248 nm

S. Gogoll [a,*], E. Stenzel [a], M. Reichling [a], H. Johansen [b], E. Matthias [a]

[a] *Fachbereich Physik, Freie Universität Berlin, Arnimallee 14, 14195 Berlin, Germany*
[b] *Max-Planck-Institut für Mikrostrukturphysik, Weinberg 2, 06120 Halle, Germany*

Received 22 May 1995

Abstract

Single-shot laser damage of polished and cleaved $CaF_2(111)$ surfaces induced by (248 nm)/(14 ns) pulses was studied by electron microscopy and probe beam deflection. It is shown that the onset of laser damage is fracturing rather than melting. The fragment thickness is found to increase with fluence which points to an enhanced near surface absorption of about 0.4 μm characteristic depth. Bending of the fragments with typical curvature radii around 100 μm indicates that within this fragment thickness a transition to plasticity has taken place.

1. Introduction

Laser damage of dielectrics with bandgaps larger than the photon energy has been intensely investigated, as documented by [1–8] and references therein. Nevertheless, the topic remains a challenge, and predictions of damage thresholds on the basis of material properties are still a far off goal. The reason for this is the complexity of the problem which sensitively depends on both target properties and laser field. The response of the material is equally important as laser pulse length, photon energy, and irradiation mode. In order to learn about the damage mechanisms, it is advisable to study one-shot (1-on-1) damage with well-defined systems like single crystals. Such investigations have been reported, e.g., for alkali halides [9,10] alkaline–earth fluorides [11–13], oxides [9,14–16], and glasses [13,17].

One question in this context is the *light absorption* for $h\nu < E_g$, where E_g is the optical bandgap of the material. Here, the purity of the crystals plays a decisive role. Impurities as well as color centers, structural defects, and surface states, all give rise to occupied states in the bandgap, and there is general agreement that these are responsible for single photon absorption [18–21]. The problem is, however, that in most cases the electronic structure of these states is not reliably known. Also, one has to carefully distinguish between single- and multi-shot irradiation of the same spot, since the defect concentration will build up during continued irradiation, a phenomenon called 'incubation' [22]. Multiphoton absorption will play a minor role in commercial materials, but becomes important in ultrapure crystals [6]. However, when visible laser light is applied to commercial crystals, multiphoton absorption resonantly enhanced by unoccupied defect states in the band gap may play a role [18,23]. Furthermore, one should keep in mind that near surface absorption may lead to photoemission, while in the bulk excited electrons in the conduction band can absorb sufficient energy for further collisional excitation of electron–hole pairs without being emitted [6].

The *material response* is governed by the degree

* Corresponding author.

SSDI 0169-4332(95)00440-8

of excitation, the crystal structure, and the electron–lattice coupling [8]. Single crystals will react differently compared to amorphous materials. Intense laser fields as realized with ultrashort pulses will cause dielectric breakdown and plasma formation [13,17]. Longer pulses might lead to melting and boiling [13]. It should be emphasized, however, that irradiation mode and energy localization determine the outcome. In multi-shot mode, the growing absorption due to accumulation of structural defects is expected to cause melting, as was verified for amorphous SiO_2 [13] and single crystalline MgO [15]. However, one or a few pulses of moderate fluence cause fracture in MgO [15]. Similarly, single crystals of alkali and alkaline–earths halides irradiated with nanosecond pulses in multi-shot mode seem to disintegrate by fracture, and no melting was reported [10,11]. Still, too few systematic microscopic investigations of the damage character have been carried out to make generalized statements.

Along these lines, we present new microscopic data on laser damage thresholds of cleaved and polished (111)-surfaces of CaF_2 single crystals. One-shot irradiations (1-on-1) were performed in air with (248 nm)/(14 ns) pulses in a fluence range between 1 and 40 J/cm^2. In all measurements, a laser beam of good top hat profile was used. Two types of measurements were done: (1) exposed spots were inspected by scanning electron microscopy, (2) damage thresholds were detected by the probe beam deflection technique.

2. Damage thresholds

Reports about multi-shot laser damage of CaF_2 can be found in the literature for various laser wavelengths and pulse durations [11,13,24–27]. Many shots on one spot, however, alter the crystal, and thresholds obtained in this way are ill-defined. Only single-shot results qualify for comparison with other materials and yield the information needed for a better understanding of the initial damage mechanism.

The question pursued in this paper is whether cleaved and polished crystals reveal a similar damage behavior. For threshold measurements of the plasma onset we employ two in-situ detection

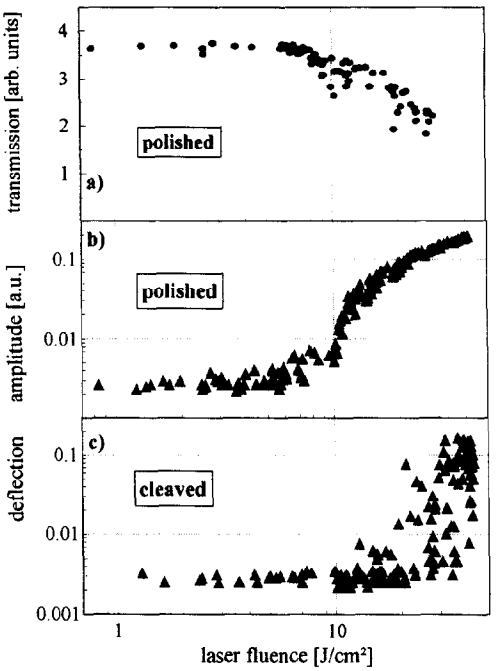

Fig. 1. Single-shot damage thresholds of polished and cleaved CaF_2(111) surfaces for irradiation with (248 nm)/(14 ns) laser pulses in air. (a) Fluence dependence of the laser light transmission. Amplitudes of the probe beam deflection are displayed for polished (b) and cleaved (c) surfaces. The irradiated spot diameter was 0.15 mm.

schemes, the change in transmission of the pump light, and the probe beam deflection (PBD) technique. The latter records the transient change in refractive index by density variations generated by heat or plasma expansion and is even sufficiently sensitive to register cracking sounds [28].

The results for a cleaved and polished surface are displayed in Fig. 1. Each data point is taken on a virgin spot. An abrupt change of deflection amplitude indicates the onset of shock waves due to the development of a plasma. The dominant result is that a polished surface (Fig. 1b) has a well-defined plasma threshold at 10 J/cm^2. The threshold for a cleaved surface (Fig. 1c) is at an average 3 times higher, but the data scatter over a fluence range from 20 to 40 J/cm^2. This result is no surprise since cleaved surfaces hold an irregular distribution of steps, the number of which varies from spot to spot over the spot diameter of 0.15 mm used in the experiments.

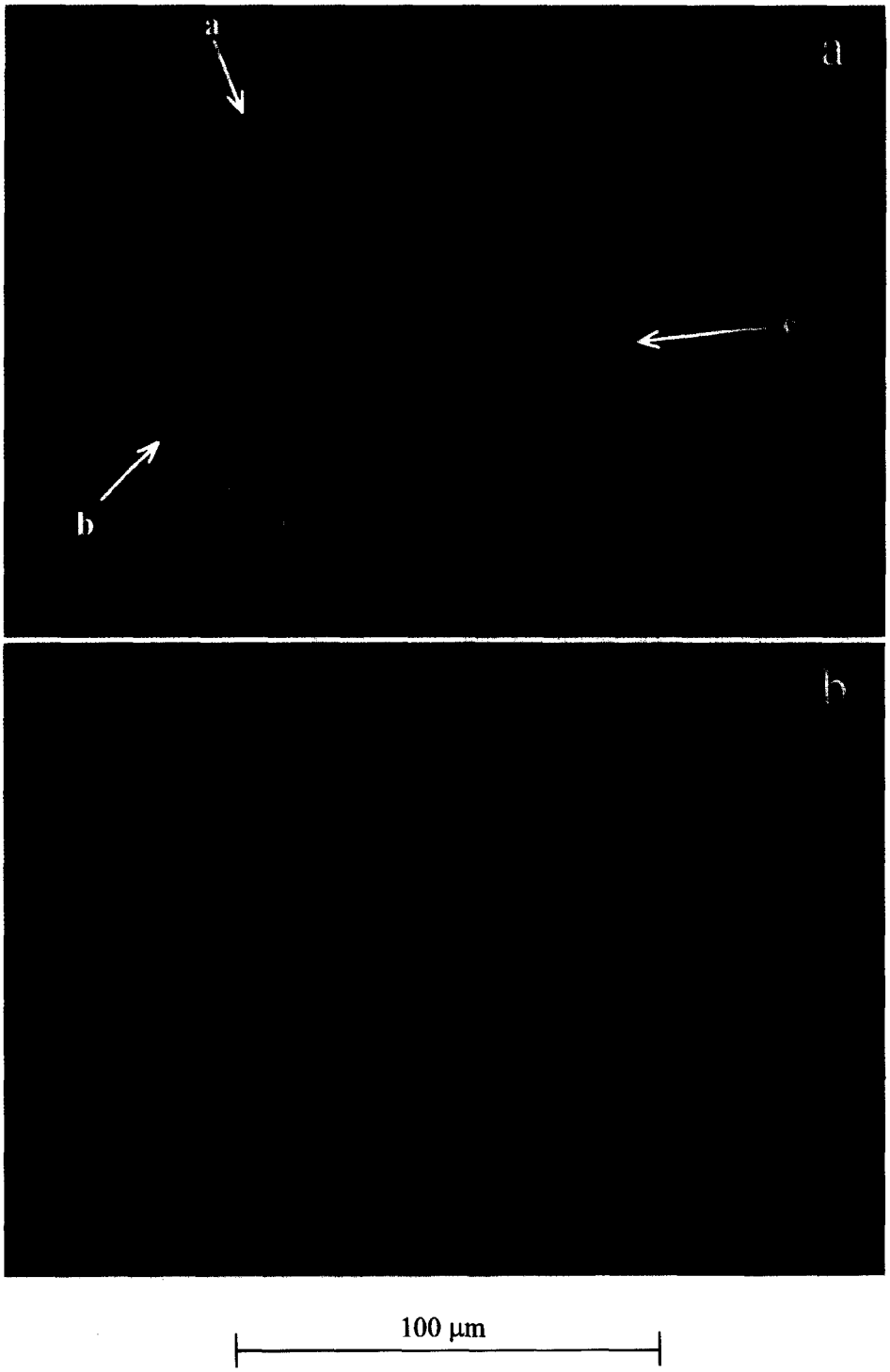

Fig. 2. Microscopic images of single-shot laser damage of polished (a), and cleaved (b) $CaF_2(111)$ surfaces generated by (248 nm)/(14 ns) laser pulses in air. The respective fluences were 36.1 J/cm^2 in (a) and 21.7 J/cm^2 in (b). The ring pattern was obtained by reflection microscopy using white light.

Since defect densities accumulate along steps [21], these can be considered as damage seeds. It would therefore be desirable to achieve a measurement on a plateau only in order to obtain the 'true' damage threshold. From the bunching of the data in Fig. 1c we estimate the damage threshold to lie around 40 J/cm^2 or higher.

A closer inspection of Fig. 1a reveals a 10% drop in transmission above 5 J/cm^2, which is caused by light scattering at microcracks that occur before the plasma develops and ablation takes place. One can also recognize that the deflection amplitude rises distinctly above this fluence. Since the PBD technique is sensitive to acoustics, we propose that this amplitude increase is due to cracking sounds, similar to what was observed previously for the rupture of brittle Cr films [28]. This interpretation is supported by electron microscopy, discussed in the next section.

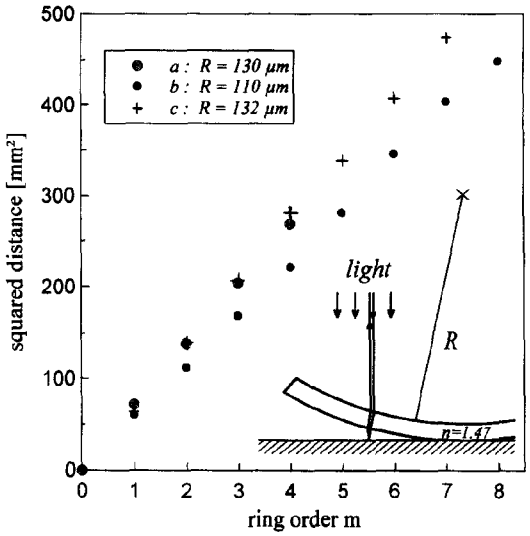

Fig. 3. Analysis of Newton's rings for the three fragments denoted by a, b, c in Fig. 2a. The inset illustrates the origin of the ring pattern. The radii of curvature for the three fragments are indicated.

3. Microscopic images

3.1. Optical microscopy

For modeling laser damage it is important to understand the material response following light absorption at defect sites. Thermal and thermoelastic response can lead to melting and boiling or, alternatively, to fracture and ejection of large scale fragments. Which path is followed depends on fluence, irradiation mode and material properties, and can be analyzed by post-irradiation optical and electron microscopy.

Fig. 2 shows two typical damage patterns on polished (Fig. 2a) and cleaved (Fig. 2b) $CaF_2(111)$ surfaces, obtained by optical reflection microscopy. Damage of the polished surface was produced by 36.1 J/cm^2, which is almost four times above the damage threshold. In case of the cleaved surface, the fluence of 21.7 J/cm^2 was more at the beginning of the threshold distribution (cf. Fig. 1c). Yet, for both surfaces the mechanism seems to be identical and involves fracture along cleavage planes and bending of the fragments. There is no indication of melting in either case.

Reflection microscopy was used to obtain Newton's ring pattern from the curved fragments. Radii of dark rings obey the relation $r = \sqrt{m\lambda R}$, where m is the order, R the radius of curvature, and λ the wavelength of the light used for observation. Since we utilized white light (to make the rings more colorful!), an averaged wavelength of $\lambda = 580$ nm was used for the analysis. Three fragments, denoted in Fig. 2a by a, b and c were analyzed, and the results shown in Fig. 3 confirm that we are indeed observing Newton's rings. This means that the curved fragments are of uniform thickness and the profile of the crystal surface beneath must be even to a fraction of a wavelength. All three fragments at the different sites in the spot shown in Fig. 2a have, within an uncertainty of 10%, a comparable curvature of $R =$ 120 μm. Up to now we found no clear evidence for a variation of R with fluence.

The scattered data on the ablation threshold of a cleaved surface in Fig. 1c raise the question of damage morphology near a step. Fig. 4 illustrates this point. Here, a cleaved surface was irradiated by a single pulse of 21 J/cm^2, the laser spot covering both the lower and higher plateau next to a step. When the microscope focuses on the lower plateau (Fig. 4a), a fracture pattern without any sign of

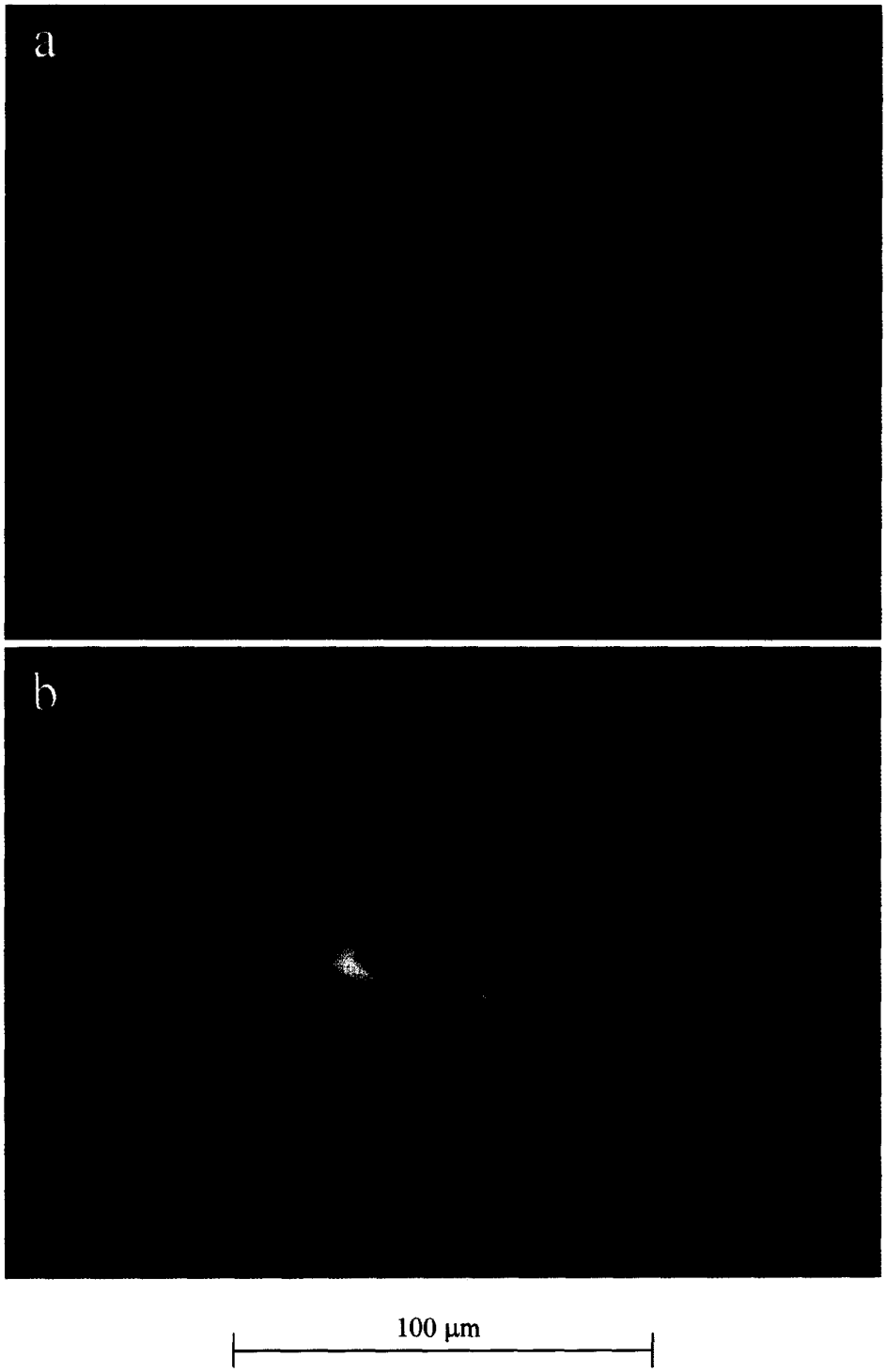

Fig. 4. Single-shot damage morphology of a cleaved $CaF_2(111)$ surface around a step. The microscope focus was placed on the lower plateau (a), and on the elevated level adjacent to the step (b). The fluence was 21 J/cm^2.

melting is observed. When focusing on the elevated plateau to the right of the step, melting can be recognized together with a high density of dislocations and/or cracks in the periphery of the irradiated spot (Fig. 4b). We attribute the different damage behavior of the upper plateau to the high density of defect states that exists at the step edge. These electronic states facilitate single photon absorption which leads to efficient heating. In consequence, the near edge region of the elevated plateau might exceed the melting temperature which is close to 1700 K. In addition, the temperature rise of the elevated plateau may be enhanced by diminishing contact with and decreasing vertical heat transport to the crystal beneath. The lower plateau contains, in comparison, much fewer light absorbing defects and is in good thermal contact to the rest of the crystal. Fracture in this part (cf. Fig. 4a) indicates that the temperature remains below the transition temperature to plasticity which manufacturers claim to be about 600°C [29]. Hence, the material response is strongly related to the surface topography.

3.2. Electron microscopy

For further analysis scanning electron microscopy (SEM) was employed. A typical damage pattern on a polished (111)-surface produced by a fluence of 27.6 J/cm^2 is displayed in Fig. 5. Again, no melting is observed and the material is removed in form of large fragments whose shape reflects the cleavage planes of the crystal. The main feature of the picture is large tiles in the center of the irradiated area and small ones at the rim. We attribute this to lateral thermal stress. Assuming an enhanced absorption in the near surface region, the top hat profile generates a large lateral thermal gradient at the rim, while there is no lateral thermal gradient in the center area. Instead, there exists a strong vertical thermal gradient. Both together give rise to shear stress and cause

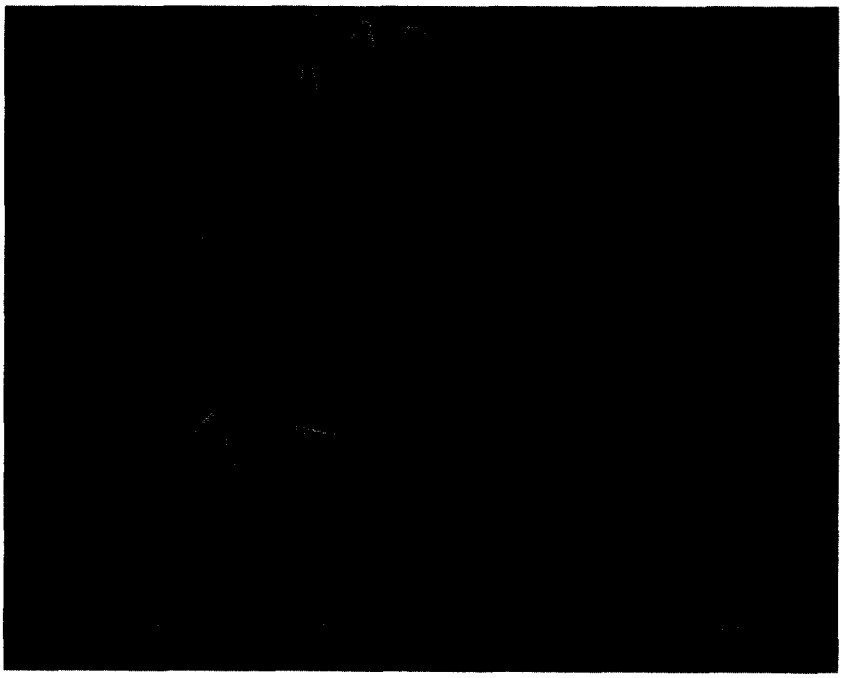

Fig. 5. Electron microscopy image of damage induced on a polished $CaF_2(111)$ surface by one laser pulse of 27.6 J/cm^2 fluence at 248 nm.

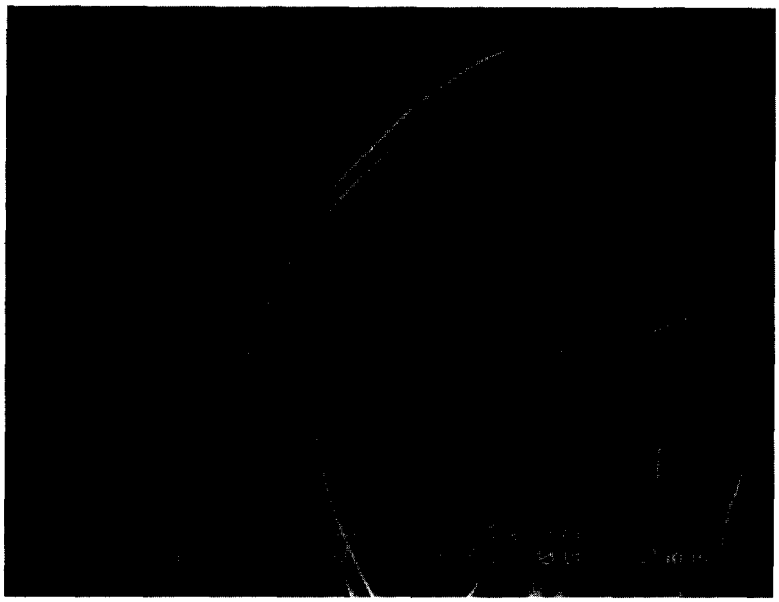

Fig. 6. SEM micrograph of $CaF_2(111)$ surface irradiated by one laser pulse of 10 J/cm^2 at 532 nm. Despite the longer wavelength damage morphology is comparable to that of 248 nm. The crystal was tilted 77° with respect to the incident electron beam thus allowing measurement of the fragment thickness.

cracking at a certain depth parallel to the surface plane and fracturing across the surface along cleavage planes. Systematic investigations of many irradiated spots on polished and cleaved surfaces reveal that fracture is in both cases the principal mechanism for single-shot damage.

In Fig. 5 the edge effect of secondary electron emission unambiguously indicates the concave curvature of individual tiles. However, this kind of micrograph allows no information about fragment thickness. For a quantitative determination of tile thicknesses SEM images were recorded under oblique angles of incidence. Fig. 6 displays an impressive example of bent fragments still partly attached to the crystal. Such images, taken with higher magnification permit stereometric measurements of tile thicknesses. For a polished surface, these are plotted in Fig. 7 as a function of laser fluence. Up to a break at around 25 J/cm^2 there is a logarithmic increase of tile thickness with fluence. The strong increase beyond this fluence points toward explosive eruptions from greater depths, possibly produced by avalanche breakdown. It is possible to describe the data assuming an enhanced absorption in the near surface range, exponentially decreasing with depth z:

$$\alpha(z) = \alpha_b + \alpha_s e^{-z/d}, \quad (1)$$

where α_b and α_s are the absorption coefficients of bulk and surface, respectively. In the following, the

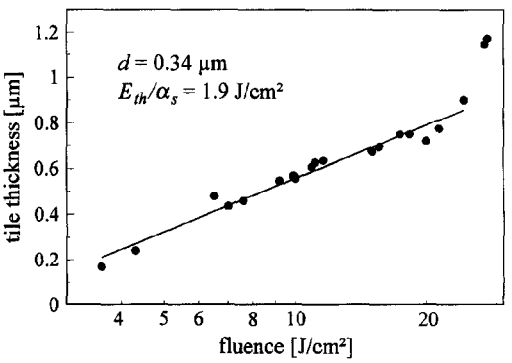

Fig. 7. Fluence dependence of fragment thickness produced by single (248 nm)/(14 ns) laser pulses on a polished $CaF_2(111)$ surface. The solid line represents a model calculation described in the text.

bulk absorption for 248 nm is neglected. The conjecture of an additional absorption within a surface layer of characteristic depth d is based on observations that polishing affects the crystalline structure. For polished CaF_2 surfaces the existence of an upper 'mosaic-crystalline' layer of 0.25 μm, followed by a 4 μm elastically deformed region was reported [30]. The near surface layer is therefore characterized by a high density of dislocations described by α_s. It is reasonable to assume that this surface absorption decreases exponentially toward the undisturbed bulk. The larger absorption of polished surfaces compared to cleaved ones was also observed on other crystals [15]. In Eq. (1) any incubation during the 14 ns laser pulse is neglected, i.e., α_s is supposed to be independent of fluence. Whether or not residues of the polishing powder that could diffuse along dislocations also contribute to the additional absorption, is an open question.

In order to accomplish fracture, a minimum volume energy density

$$E_{th} = \alpha(l) F_{th}(l) \tag{2}$$

must be absorbed which defines a characteristic depth l, that can be written in the form:

$$l = d \ln(\alpha_s F / E_{th}). \tag{3}$$

We identify this depth with the observed fragment thickness. The logarithmic increase of the fragment thickness in Fig. 7 supports this assumption. A fit to the data represented by the solid line yields $d = 0.34$ μm and $F_{th} = 1.9$ J/cm^2. The latter value amounts to about 1/5 of the plasma threshold in Fig. 1b. This means that fracture starts at fluences where the particle emission is still too small for plasma ignition.

Using (2) we can obtain from the threshold fluence for fragmentation, F_{th}, a rough estimate of the surface absorption coefficient. Following Orowan [31], the energy density necessary for separating two adjacent CaF_2 layers in the (111) plane is proportional to the surface tension $\gamma(111)$:

$$E_{th} = \gamma(111)/\Delta. \tag{4}$$

Here, $\Delta = a/\sqrt{3}$ is the spacing between the two neighboring planes. The surface tension of CaF_2 was measured by Gilman [32] to be $\gamma(111) = 45 \times 10^{-6}$ J/cm^2. With the lattice constant $a = 5.46$ Å, we find $E_{th} \approx 1400$ J/cm^3, resulting in $\alpha_s \approx 760$ cm^{-1}. Combined with the thickness of the defect layer obtained from the data in Fig. 7, we find that the enhanced surface absorption amounts to $\alpha_s d \approx 3\%$.

This simple model describes the experimental data in Fig. 7 surprisingly well and leads to a reasonable value of α_s. The model has two weak points, however. One concerns the validity of Eq. (4) [31]. The other is the fluence independence of α_s, which excludes incubation effects during the 14 ns laser pulse. A possible reason for this may be a slow growth rate of dislocations. Certainly, these points need further investigation.

The model is further supported by the concave bending of the fragments (cf. Figs. 2 and 3). An enhanced absorption in a surface layer, exponentially decreasing with depth, causes a similar temperature profile throughout this layer. The crystal, however, turns ductile above 600°C [29]. When the temperature near the surface is sufficient to reach plasticity while the deeper part of the fragment remains brittle, shear stress will bend the fragments upward.

4. Summary and conclusion

Single-shot laser damage of CaF_2(111) surfaces, irradiated by (248 nm)/(14 ns) pulses in air, has been studied on cleaved and polished surfaces. Probe beam deflection measurements show, that polished crystals exhibit a well-defined plasma onset at 10 J/cm^2, while the threshold values for cleaved surfaces scatter over a fluence interval between 20 and 40 J/cm^2 (Fig. 1). This scatter is caused by the number of steps that happen to be located in the irradiated spot.

Optical and electron microscopy shows that the damage mechanism is identical for cleaved and polished surfaces in the investigated fluence range. Initial damage is dominated by fracture and ejection of large fragments (Figs. 2 and 4, and Fig. 5). The fragments are bended and the radius of curvature was measured to be about 120 μm (Fig. 3). For the fluences used, melting seems to occur only on cleaved surfaces at the upper edges of steps (Fig. 4), where a high defect density increases absorption, and fading contact to the bulk crystal hinders heat conduction. This is consistent with the observation [13] that melting plays a bigger role for multi-shot damage.

The fragment thickness was found to vary with fluence for polished surfaces. This variation can be explained by a simple model based on an enhanced absorption in a surface layer of 0.34 μm thickness. This value is in accord with reports about the damage depth produced by polishing. The absorption increase within this layer comes out to be about 3%. The model assumes an exponentially decreasing absorption with increasing depth. The corresponding temperature distribution may be the cause for the bending of the fragments. Nevertheless, the model needs further testing.

Acknowledgements

This work was supported by Deutsche Forschungsgemeinschaft, Sfb 337.

References

[1] M. von Allmen, Laser-Beam Interactions with Materials, Springer Ser. Mater. Sci. 2 (Springer, Berlin, 1987).
[2] R.M. Wood, Ed., Laser Damage in Optical Materials (SPIE Optical Engineering Press, Bellingham, WA, 1990).
[3] E. Fogarassy and S. Lazare, Eds., Laser Ablation of Electronic Materials (Elsevier, Amsterdam, 1992).
[4] J.C. Miller and D.B. Geohegan, Eds., Laser Ablation: Mechanisms and Applications-II, AIP Conf. Proc. No. 288 (AIP, New York, 1994).
[5] J.C. Miller, Ed., Laser Ablation, Springer Ser. Mater. Sci. 28 (Springer, Berlin, 1994).
[6] S.C. Jones, P. Braunlich, R.T. Casper, X.-A. Shen and P. Kelly, Opt. Eng. 28 (1989) 1039.
[7] N. Itoh, K. Tanimura and Y. Nakai, Nucl. Instr. Meth. B 65 (1992) 21.
[8] R.F. Haglund, Jr. and R. Kelly, Mater.-Fys. Medd. 43 (1993) 527.
[9] R.F. Haglund, Jr., M. Affatigato, J.H. Arps and K. Tang, Nucl. Instr. Meth. B 65 (1992) 206.
[10] R.L. Webb, L.C. Jensen, S.C. Langford and J.T. Dickinson, J. Appl. Phys. 74 (1993) 2338.
[11] M. Reichling, H. Johansen, S. Gogoll, E. Stenzel and E. Matthias, Nucl. Instr. Meth. B 91 (1994) 628.
[12] O. Kreitschitz, W. Husinsky, G. Betz and N.H. Tolk, Appl. Phys. A 58 (1994) 563.
[13] B.C. Stuart, M.D. Feit, A.M. Rubenchik, B.W. Shore and M.D. Perry, Phys. Rev. Lett. 74 (1995) 2248.
[14] M.A. Schildbach and A.V. Hamza, Phys. Rev. B 45 (1992) 6197.
[15] R.L. Webb, L.C. Jensen, S.C. Langford and J.T. Dickinson, J. Appl. Phys. 74 (1993) 2323.
[16] J.T. Dickinson, S.C. Langford, J.J. Shin and D.L. Doering, Phys. Rev. Lett. 73 (1994) 2630.
[17] D. Du, X. Liu, G. Korn, J. Squier and G. Mourou, Appl. Phys. Lett. 64 (1994) 3071.
[18] E. Matthias and T.A. Green, Springer Ser. Surf. Sci. 19 (1990) 113.
[19] K. Tanimura and N. Itoh, Nucl. Instr. Meth. B 46 (1990) 207
[20] E. Westin, A. Rosén and E. Matthias, Springer Ser. Surf. Sci. 19 (1990) 316.
[21] J.T. Dickinson, Nucl. Instr. Meth. B 91 (1994) 634.
[22] E. Sutcliffe and R. Srinivasan, J. Appl. Phys. 60 (1986) 3315.
[23] J. Reif, Opt. Eng. 28 (1989) 1122.
[24] R.C. Estler, E.C. Apel and N.S. Nogar, J. Opt. Soc. Am. B 4 (1987) 281
[25] J. Reif, S. Petzoldt, A.P. Elg and E. Matthias, Appl. Phys. A 49 (1989) 199.
[26] R. Mitzner, A. Rosenfeld and R. König, Appl. Surf. Sci. 69 (1993) 180.
[27] E. Matthias, S. Gogoll, E. Stenzel and M. Reichling, Rad. Eff. Def. Solids 128 (1994) 67.
[28] E. Matthias, J. Siegel, S. Petzoldt, M. Reichling, H. Skurk, O. Käding and E. Neske, Thin Solid Films 254 (1995) 139.
[29] Harshaw/Bicron Crystal Products, Technical Notes.
[30] B. Dietrich, E. Förster and R. Böttger, Krist. Tech. 12 (1977) 609.
[31] E. Orowan, Rep. Progr. Phys. XII (1948/49) 185.
[32] J.J. Gilman, J. Appl. Phys. 31 (1960) 2208.